Journal of Materials Chemistry A

PAPER

View Article Online
View Journal | View Issue

Cite this: J. Mater. Chem. A, 2018, 6, 7913

Germanium-incorporated lithium silicate composites as highly efficient low-temperature sorbents for CO_2 capture

P. V. Subha,[a] Balagopal N. Nair,*[bc] V. Visakh,[a] C. R. Sreerenjini,[a] A. Peer Mohamed,[a] K. G. K. Warrier,[a] T. Yamaguchi[d] and U. S. Hareesh *[ae]

Received 18th January 2018
Accepted 3rd April 2018

DOI: 10.1039/c8ta00576a

rsc.li/materials-a

Carbon dioxide emission from massive point sources such as industries and power plants is perceived to be a major contributor towards global warming and associated climate changes. Although lithium silicate has the highest capacity for CO_2 sorption (8 mmol g^{-1}), it is kinetically limited during the sorption process, particularly at temperatures below 500 °C. Herein, we report a facile strategy for the development of germanium-incorporated lithium silicate composites, which display enhanced CO_2 absorption capacity as well as kinetics in the temperature range of 150–680 °C. The absorption capacity of 324 mg g^{-1} at the rate of 117 mg g^{-1} min^{-1} was measured at 680 °C, and 49 mg g^{-1} at the rate of 36 mg g^{-1} min^{-1} was measured at 300 °C for samples with a Si : Ge molar ratio of 1 : 0.183. This study thus highlights the possibility of employing germanium-incorporated lithium silicates for the absorption of CO_2 at a wide range of temperatures, including the *in situ* removal of CO_2 from chemical and petrochemical reactions, such as the water–gas shift reaction occurring at low temperature ranges of 150–450 °C, that has hitherto been not possible with pure Li_4SiO_4.

1. Introduction

The atmospheric concentration of CO_2 has dramatically increased in the post-industrial era and has reached the present value of approximately 400 ppm. This has, in turn, created severe environmental issues such as global warming and climate destabilization, inducing undesirable weather patterns and natural calamities. For sustainable balance of the carbon cycle in the biosphere, selective and controlled removal of CO_2 followed by its reuse or sequestration is essential. It is, therefore, necessary to develop sustainable technologies for the effective removal of CO_2 from the point sources to reduce carbon footprints in the atmosphere.[1–15] In order to realize this, most often, we rely on post-combustion CO_2 capture and proven approaches such as the use of amine-based absorbents and oxy-combustion techniques that are adopted to reduce the increasing level of CO_2 in the atmosphere.

Out of various high-temperature CO_2 absorbents[16–18] currently available, Li_4SiO_4 qualifies as a potential material by virtue of its high absorption capacity with appreciable kinetics at elevated temperatures (450–700 °C).[19–23] However, the drawbacks of using Li_4SiO_4 are its poor absorption capacity and slow kinetics in the low-temperature range (150–450 °C), where several chemical and petrochemical reactions occur. This necessitates the need for the development of materials that display appreciable absorption capacities at lower temperatures. Conventionally synthesized lithium silicate materials[24,25] in the pure form absorb CO_2 in the temperature range of 650–700 °C. Nevertheless, the kinetics are affected due to strong lattice enthalpy and diffusion resistance arising from the absorption product layer. The addition of second phase eutectics can promote CO_2 absorption at lower temperatures to some extent. Several synthesis approaches such as sol–gel, hydrothermal, thermal oxidation, and plasma irradiation have been adopted to control the morphology and composition of the lithium silicate particles.[26–28] The solid-state approaches often use high calcination temperatures, which lead to particle agglomeration and non-uniform particle size distributions. Wet chemical approaches such as hydrothermal or co-precipitation are effective in morphological control but are time-consuming. Radiative techniques such as plasma oxidation[29,30] have recently been used for the preparation of Li_4SiO_4. However, the use of high temperature can induce compositional changes

[a]Materials Science and Technology Division (MSTD), National Institute for Interdisciplinary Science and Technology, Council of Scientific and Industrial Research (CSIR-NIIST), Pappanamcode, Thiruvananthapuram, Kerala 695019, India. E-mail: hareesh@niist.res.in; ushareeshnair@gmail.com

[b]R&D Centre, Noritake Company LTD, 300 Higashiyama, Miyoshi, Aichi 470-0293, Japan. E-mail: bnair@n.noritake.co.jp

[c]School of Molecular and Life Sciences (MLS), Faculty of Science and Engineering, Curtin University, GPO Box U1987, Perth, Western Australia 6845, Australia

[d]Chemical Research Laboratory, Tokyo Institute of Technology, RI-17, 4259 Nagatsuda-cho, Midori-ku, Yokohama 226-8503, Japan

[e]Academy of Scientific and Innovative Research, Delhi-Mathura Road, New Delhi 110 025, India

due to the sublimation of lithium during irradiation, which leads to poor absorption and kinetics during the sorption process. We have previously reported the synthesis of Li_4SiO_4 through a microwave-assisted sol–gel process, resulting in the formation of Li_4SiO_4 nanorods that displayed near theoretical absorption capacity with enhanced sorption rates.[31,32] However, the CO_2 absorption properties of the pure Li_4SiO_4 powder were found insignificant below 450 °C.

In the present investigation, we aim to enhance the kinetics and absorption capacity of Li_4SiO_4 material at low as well as elevated temperatures through the development of germanium-incorporated Li_4SiO_4 nanostructures. Because silicon and germanium exhibit similar physical and chemical properties, substitution of silicon by germanium is possible, due to lattice expansion, and thereby an increase of CO_2 absorption is expected. Germanium compounds exhibit higher electronic conductivity and lithium diffusivity than that of silica, but its lack of economic viability imposes restrictions for widespread applications. Fuller and Severiens revealed that lithium has the ability to migrate as a singly charged positive ion in single crystals of both Ge and Si in the temperature ranges of 150–600 °C and 360–860 °C, respectively.[33] Furthermore, Graetz *et al.* reported that lithium ion diffusivity in Ge matrices is approximately 15 times higher than that of silica at 360 °C and can hence be used in lithium batteries.[34] In view of such favourable diffusion properties of germanium, it is expected that the lithium ion hopping in germanium-containing lithium silicate structures should be larger than that of the Li_4SiO_4 matrices. It is also known that Li_4SiO_4 and Li_4GeO_4 are iso-structural. Hence, the incorporation of germanium in the crystal lattice of Li_4SiO_4 could be considered as an option to process high-performance absorbent materials. Togashi *et al.* compared the absorption capacity of Li_4TiO_4, Li_4SiO_4, and Li_4GeO_4; however, their results showed that the absorption performance of Li_4GeO_4 in its pure form is lower than that of Li_4TiO_4 [35] and Li_4SiO_4.[36,37]

In the current study, the possibility of employing germanium-substituted Li_4SiO_4 for the absorption of CO_2 at temperatures as low as 150 °C is demonstrated for the first time. Moreover, the sorbent structure is tailored to be nanosized to minimize diffusion resistance during the CO_2 capture as well as during its regeneration. The present investigation thus reveals the development of germanium-incorporated lithium silicate (Ge-LS) for the reactive absorption of CO_2. By employing a microwave sol–gel approach, we constructed nanorods of substituted structures that displayed enhanced CO_2 absorption with significantly improved kinetics at low as well as elevated temperatures.

2. Experimental

a. Synthesis of germanium-incorporated lithium silicate

$Li_4Si_xGe_{1-x}O_4$ with Si : Ge molar ratios of 1 : 0.040, 1 : 0.084, 1 : 0.183, and 1 : 0.447 was synthesized by a sol–gel method employing lithium nitrate (Alfa Aesar, USA), colloidal silica (purity 99.8%, Aldrich Chemicals, USA) and germanium tetrachloride (Alfa Aesar, USA) as the starting precursors. Initially, 11.495 g of lithium nitrate dissolved in 40 ml of distilled water was hydrolysed by the slow addition of ammonium hydroxide solution, and the pH was raised to 8. Subsequently, colloidal silica and germanium tetrachloride were added drop wise to this reaction mixture with constant stirring. The resulting sol was then subjected to microwave irradiation for 4 min, dried at 150 °C for 15 h, and calcined at 800 °C for 3 h to obtain germanium-incorporated lithium silicate (Ge-LS).

The phase-pure lithium silicate (Li_4SiO_4) sample for comparison was also made by the sol–gel method, starting from lithium nitrate and colloidal silica as precursors. For this, lithium nitrate (11.495 g) was dissolved in 40 ml distilled water, and by the slow addition of ammonium hydroxide solution (25%, s. d. Fine-Chem. Ltd, India), the pH was increased to 8 with constant stirring. Furthermore, 8.5 g of colloidal silica sol (50 wt%, purity 99.8%, Aldrich Chemicals, USA) was added dropwise to the reaction mixture. The mixed sol thus obtained was subjected to microwave irradiation for 2 min followed by oven drying at 150 °C for 15 h. The mixture was calcined at 800 °C for 3 h to obtain a phase-pure lithium silicate sample.

b. Characterisation

The crystalline phases of the synthesized samples were analysed by employing X'pert Pro diffractometer, (Philips, Eindhoven, The Netherlands) and SAXS/WAX system (Xeuss Xenocs, France) in the 2θ range of 15–36° using Cu Kα radiation (λ = 0.154 nm). Raman spectra of pure and germanium-added lithium orthosilicate samples were recorded using a WI-Tec Raman microscope (WI-Tec, Inc., Germany, Alpha 300R) with a Peltier-cooled CCD detector. A 633 nm excitation wavelength laser was used for the excitation of the sample, and the spectra were collected in the range of 400–3000 cm^{-1} with 1 cm^{-1} resolution. The morphological and microstructural analyses of the materials were carried out using a scanning electron microscope (JEOL JSM-35) operated at 15 kV. The morphology and topographical data of the samples were investigated using high resolution-transmission electron microscopy (HR-TEM, FEI Tecnai 30G2 S-T win) with operation at 300 kV. The thermogravimetric analysis of the prepared samples was performed using a PerkinElmer STA 6000 instrument (The Netherlands) in the temperature range of 50–900 °C at a heating rate of 10 °C min^{-1}. In the setup used, the actual temperatures close to the sample were typically 5–10 °C lower than the set temperatures. The CO_2/nitrogen flow rate through the sample chamber was approximately 50 ml min^{-1}. X-ray photoelectron spectroscopy (XPS) was carried out with a PHI 5000 Versa Probe II with a monochromated Al-Kα X-ray source.

3. Results and discussion

During the microwave sol–gel process, lithium hydroxide formation occurs due to the hydrolysis of aqueous lithium nitrate.

$$LiNO_3 + NH_4OH \rightarrow LiOH + NH_4NO_3 \quad (1)$$

The addition of germanium chloride to the reaction mixture results in the formation of germanium hydroxides, as reported in the literature.[38]

$$GeCl_4 + H_2O \rightarrow Ge(OH)Cl_3 + HCl \quad (2)$$

Hydrolysed products in the reaction mixture undergo polycondensation reactions with silica, leading to the formation of the gel network. The calcination at 800 °C results in the formation of LS and Ge-LS samples. Structural and morphological as well as CO_2 absorption studies of the as-synthesized samples were carried out and are described in the following sections.

X-ray diffraction patterns of Ge-LS samples synthesized through the sol–gel route at different molar concentrations are shown in Fig. 1.

The expected characteristic reflection peaks of monoclinic lithium silicate phases were observed in all (Si : Ge) compositions; the major reflections from the planes ($\bar{1}10$), (011), and (200) with the 2θ angles of 22.1, 22.6, and 33.8, respectively, were seen and are in accordance with JCPDS (037-1472) data. The addition of germanium to the lithium silicate sample resulted in the slight shifting of the maximum intensity peak towards the lower 2θ values, compared to that of the Li_4SiO_4 sample. The peak shift can presumably be attributed to the substitution of silicon by germanium in the crystal lattice of Li_4SiO_4, leading to a lattice expansion in accordance with Vigard's law. The peak shifts in the Ge-LS samples are highlighted in the XRD patterns provided in Fig. 2.

The XRD patterns in Fig. 1 and 2 of the composition containing the highest amount of germanium (1 : 0.447) clearly revealed that other phases of germanium ($Li_4Ge_5O_{12}$) coexisted along with the lithium silicate phase. The identification of such phases was performed in conjunction with the Raman spectroscopic analysis (Fig. 3).

The characteristic vibrational frequencies of GeO_4 tetrahedra were found in the range of 850–650 cm^{-1}, and the external modes of GeO_4 were found below 370 cm^{-1}. In pure LS, the characteristics peaks are seen at wave numbers of 1086, 822, 163, and 95 cm^{-1}. The addition of germanium to the Li_4SiO_4 resulted in the slight shift of the peak at 822 cm^{-1} to the lower wavelength region due to the substitution of silicon by germanium in the crystal lattice of Li_4SiO_4 (Fig. 3). In the sample with silicon and germanium in the molar ratio of 1 : 0.040, apart from the peak shift to the left, the splitting of peaks was also observed at 829 cm^{-1}. As the germanium content was increased, the shifts corresponding to the molar ratio of 1 : 0.084 and 1 : 0.183 were 791 and 789 cm^{-1}, respectively. At the highest composition (1 : 0.447), the peak intensity at 822 cm^{-1} decreased due to the decrease in silica content in contrast to the increasing intensity of the 1093 cm^{-1} band, indicating silica substitution with germanium or the formation of the higher phase of lithium germanates in the samples.

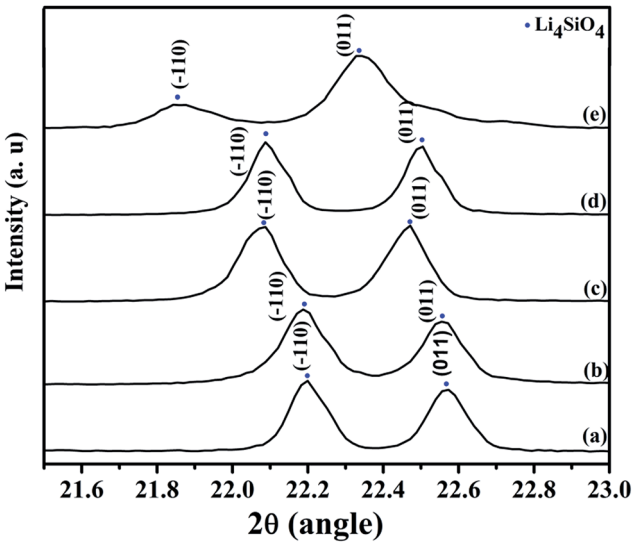

Fig. 2 X-ray diffraction patterns of (a) pure Li_4SiO_4 and (b) Ge-LS samples with different (Si : Ge) molar ratios of 1 : 0.040, (c) 1 : 0.084, (d) 1 : 0.183, and (e) 1 : 0.447.

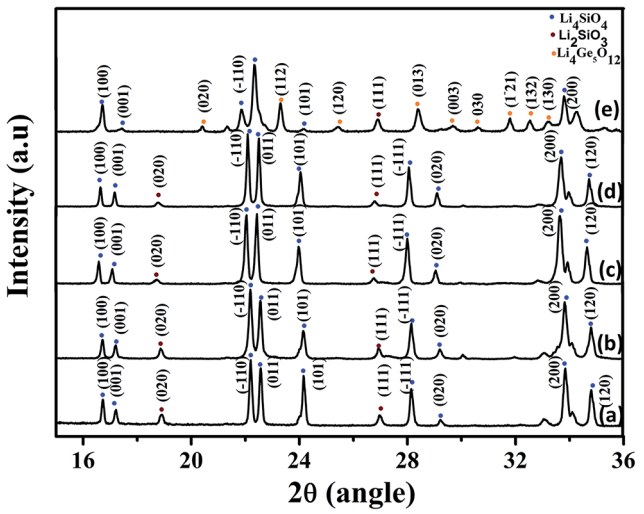

Fig. 1 X-ray diffraction patterns of (a) pure Li_4SiO_4 and (b) Ge-LS samples at different (Si : Ge) molar ratios of 1 : 0.040, (c) 1 : 0.084, (d) 1 : 0.183, and (e) 1 : 0.447.

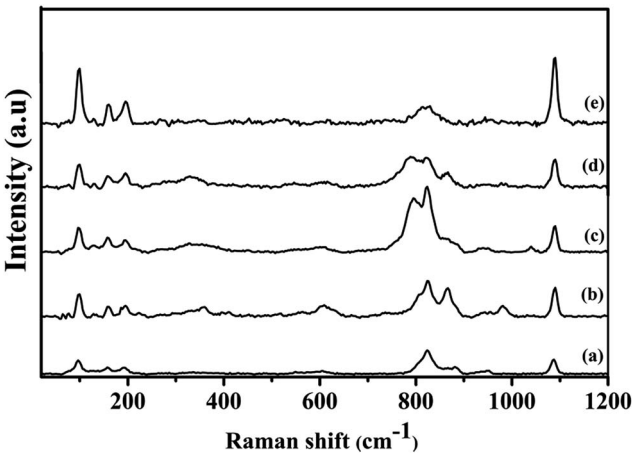

Fig. 3 Raman spectrum of (a) pure Li_4SiO_4 and (b) Ge-LS samples with different (Si : Ge) molar ratios of 1 : 0.040, (c) 1 : 0.084, (d) 1 : 0.183, and (e) 1 : 0.447.

The substitution of silicon by Ge in the crystal lattice of Li_4SiO_4 was again confirmed by the XPS spectral analysis shown in Fig. 4a and b. In Fig. 4a, the main peak of Ge $2p^{3/2}$ appeared at 1224 eV, which is related to Ge^{4+}, and the loss feature may be observed between the spin components at 1235 eV and is consistent with previously reported results.[39] The Fig. 4b XPS spectrum was deconvoluted to three peaks to fit the O 1s spectra, corresponding to Ge–O (+4), Si–O, and O–O. The peak of O 1s appearing at 531.3 eV was related to the Ge–O bond, and the core level shift of the oxidation state at 532.1 eV corresponded to the Si–O bond. The conformation of localized oxygen arising from the O–O scattering was observed at approximately 530.5 eV.

Morphological characterization of the pure LS and Ge-LS samples with the molar ratios of 1 : 0.040, 1 : 0.084, 1 : 0.183, and 1 : 0.447 are presented in Fig. 5. Morphological observations indicate that in the sample containing lower amounts of germanium (1 : 0.040), the particles exhibited flower-like morphology (Fig. 5a). In samples having the molar ratio of 1 : 0.084, the particles appeared uniformly as stacked sheets (Fig. 5b), and as the molar ratio was further increased (1 : 0.183), the particles appeared as needle-shaped structures with a lesser degree of agglomeration (Fig. 5c). Samples with an even higher concentration of Ge (1 : 0.447) showed larger particles with needle-shaped morphology (Fig. 5d).

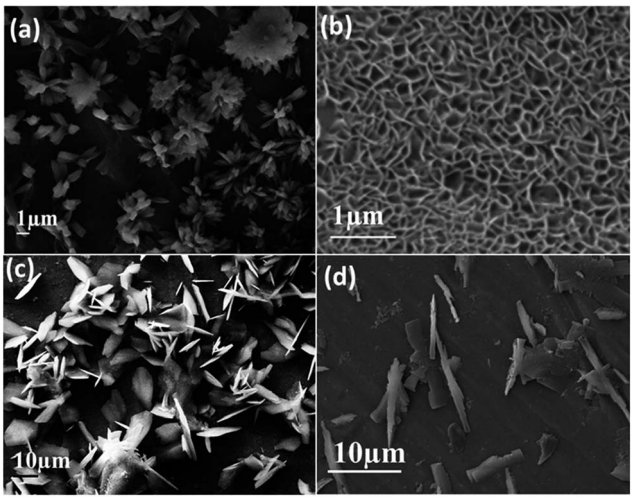

Fig. 5 SEM images of Ge-LS samples with different molar compositions of Si : Ge: (a) 1 : 0.040, (b) 1 : 0.084, (c) 1 : 0.183, and (d) 1 : 0.447.

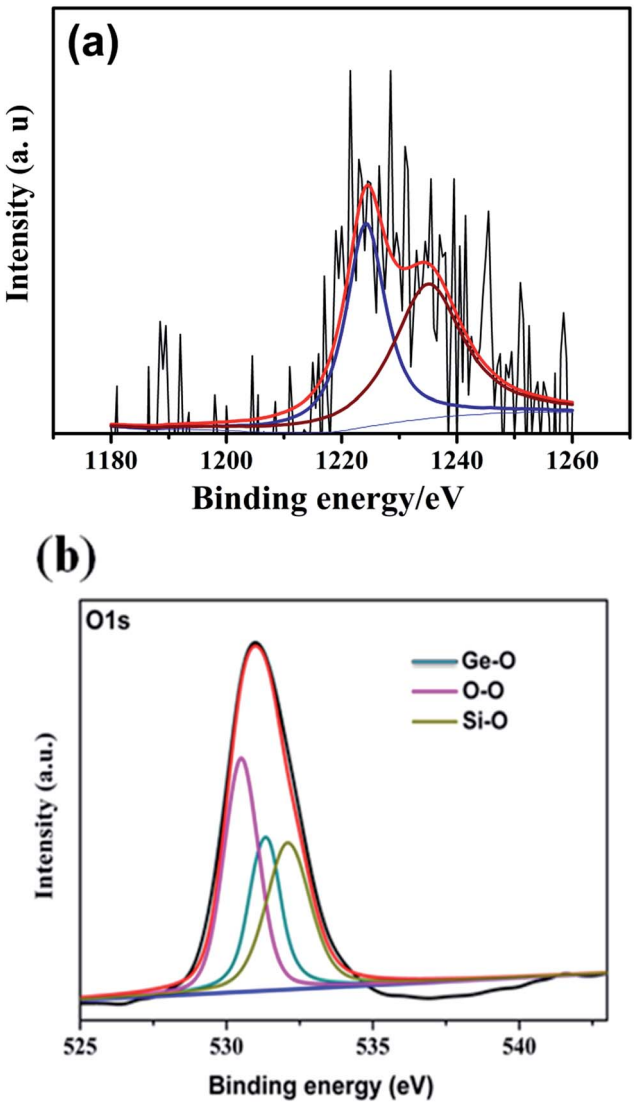

Fig. 4 XPS analysis of a Ge-LS sample in the molar ratio of 1 : 0.183. (a) Ge 2p core level spectra and (b) O 1s core level spectra of oxide formation.

Micrographs of samples containing low molar concentration (1 : 0.084) of germanium indicated that the needle formation was less apparent in such samples. The presence of Ge in these samples was confirmed from energy-dispersive X-ray analysis (EDAX), as presented in Fig. 6. Although some differences between the molar composition used for synthesis and the measured composition were detected, the EDAX results more or less reflect the synthesis composition (Table 1).

The morphology and microstructure of the samples with the molar ratio of 1 : 0.183 and 1 : 0.084 were investigated using HR-TEM, and the images are shown in Fig. 7a and b. The high magnification images show that the particles have needle structures with pointed edges, as had been revealed by the SEM images.

a. CO_2 absorption studies

CO_2 absorption studies were carried out by gravimetric techniques using thermogravimetric analysis (TGA) in the temperature range of 100–800 °C. In the sample chamber, CO_2/N_2 flow rates were approximately 50 ml min^{-1}. The mechanism of CO_2 absorption in Li_4SiO_4 is well known and has been widely reported. Absorption of CO_2 in the case of the Ge-LS sample also leads to the formation of lithium metasilicate and carbonate phases, and the reaction could be represented in the following generalized form:

$$Li_4MO_4 + CO_2 \rightarrow Li_2MO_3 + Li_2CO_3 \quad (3)$$

where $M = Si_xGe_{1-x}$.

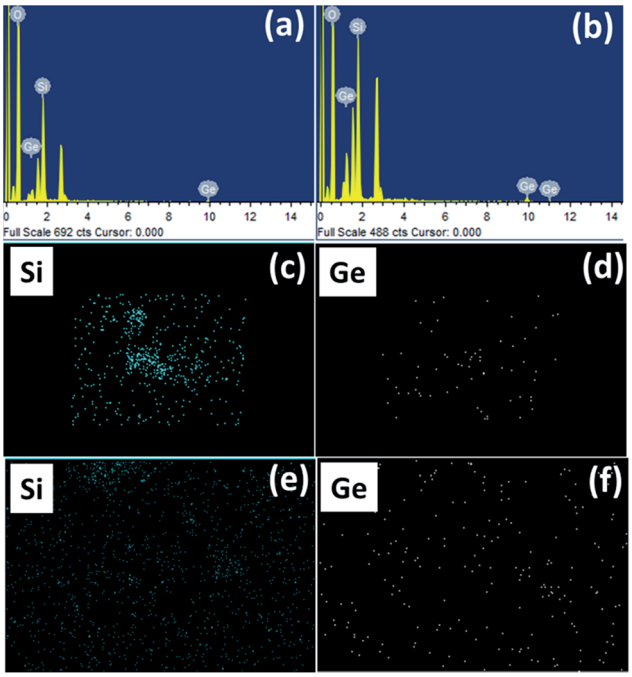

Fig. 6 (a) EDAX of the Ge-LS sample in the molar ratio of 1 : 0.084 and its elemental mapping in (c and d). (b) EDAX of the Ge-LS sample in the molar ratio of 1 : 0.183 and its elemental mapping in (e and f).

Table 1 EDAX analysis of the Ge-LS samples with different molar composition

Sl. no	Molar composition of (Si : Ge) (as per the composition used for synthesis)	Measured molar composition of (Si : Ge) (EDAX analysis of samples)
1	1 : 0.040	1 : 0.029
2	1 : 0.084	1 : 0.077
3	1 : 0.183	1 : 0.116
4	1 : 0.447	1 : 0.244

Ge-LS samples of molar ratios 1 : 0.040, 1 : 0.084, 1 : 0.183, and 1 : 0.447 were initially heated to a temperature of 800 °C at a heating rate of 20 °C min^{-1} under 100% CO_2 flow to obtain a dynamic thermogram. The dynamic thermograms of these

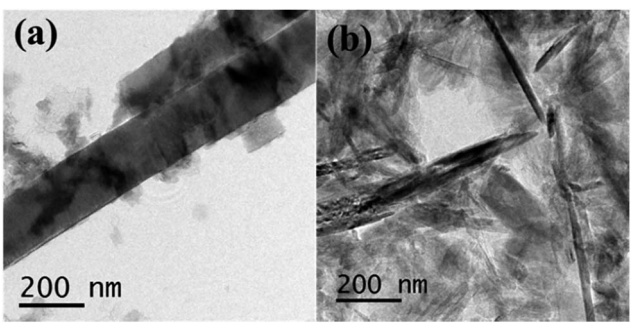

Fig. 7 TEM images of Ge-LS samples with the molar ratio of (a) 1 : 0.183 and (b) 1 : 0.084.

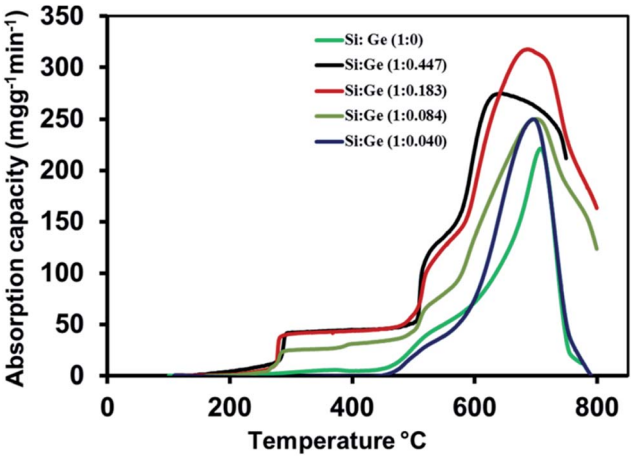

Fig. 8 Dynamic thermogravimetric analysis of germanium-incorporated lithium silicate samples measured at 20 °C min^{-1} (100% CO_2) with respect to temperature.

samples are shown in Fig. 8, and the low-temperature absorption behaviour is highlighted in Fig. 9. The absorption of CO_2 in LS became significant only after the temperature reached 500 °C; the kinetics of absorption were always negligible below 500 °C. Compared to this, Ge-LS materials exhibited four distinct absorption steps during the sorption process. CO_2 absorption was initiated at the very low temperature of 150 °C, as clearly visible from the low-temperature absorption area highlighted in Fig. 9. When the temperature was slightly above 250 °C, a sudden weight increment occurred. After the completion of this step, two more distinct steps at approximately 500 °C and 600 °C were visible in the dynamic TG patterns. Finally, as the temperature reached approximately 680 °C, the desorption of CO_2 from the samples occurred due to the reverse reaction forming the initial Ge-LS phase. The comparative absorption rates depended a great deal on the composition of the samples. The absorption capacity increased with increasing germanium addition up to the Si : Ge molar ratio of (1 : 0.183). As the Si : Ge molar ratio was increased to 1 : 0.447, the absorption capacity in the higher temperature

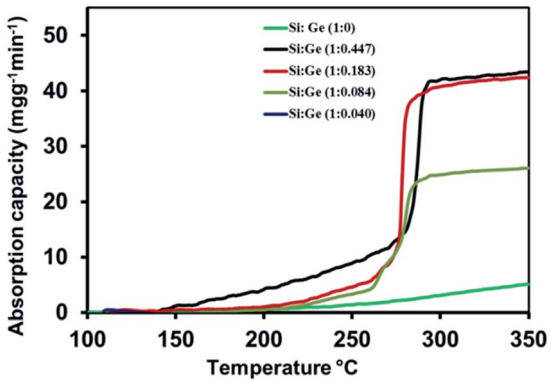

Fig. 9 Dynamic thermogravimetric analysis of Ge-LS samples in the temperature range of 100–350 °C.

range above 600 °C was reduced. As shown, Ge-LS samples exhibited significant CO_2 absorption at very low temperatures of 150 °C. The absorption of CO_2 at low temperatures increased with the increase in the concentration of germanium in the lithium silicate samples.

In the present investigation, a sample with the molar ratio of 1 : 0.183 (Si : Ge) exhibited enhanced absorption capacity and kinetics at both low and elevated temperatures compared to samples with molar ratios of 1 : 0.084 and 1 : 0.040. The sample with a molar ratio of 1 : 0.447 showed similar absorption properties with that of the sample of molar ratio of 1 : 0.183, at low temperatures. However, the absorption capacity of such samples was lower at elevated temperatures. The variation in absorption capacity at different molar ratios of silicon and germanium can be clearly correlated to the phase composition, as analyzed through XRD and Raman spectroscopy. The low absorption values observed at elevated temperatures could lead to the conclusion that at higher concentrations, excess unsubstituted germanium appears as oxide phases, resulting in a reduction of absorption capacity. For example, the formation of the $Li_4Ge_5O_{12}$ phase in the sample of Si : Ge at a (1 : 0.447) molar composition could effectively reduce the CO_2 absorption capacity, as the Li : M (Ge) ratio in this material is 4 : 5 compared to the value of 4 : 1 in Li_4SiO_4. The appreciable absorption capacity of 1 : 0.447 and 1 : 0.183 Si : Ge samples at low temperatures should be due to the presence of the germanium-incorporated lithium silicate phase.

The enhancement in the kinetics of the CO_2 absorption capacity while exposing the Ge-LS sample (1 : 0.183) to temperatures >150 °C should be mainly due to the incorporation of Ge into the lattice of lithium silicate. It has been reported that the diffusivity of lithium in germanium is 15 times higher than that of lithium in silicon at 360 °C.[34] Hence, the substitution of Si by Ge in the Ge-LS samples should have influenced the diffusion kinetics of lithium ion in the substituted silicates. Moreover, the needle-like morphology of the samples obtained by the microwave sol–gel process should also have contributed to the enhancement of the absorption kinetics, as has been reported in a recent study on phase-pure lithium silicate.[32]

Generally, low-temperature absorption (approximately 400 °C) is observed in lithium silicate samples modified with low-melting fluxes. In the present work, we have successfully enhanced the kinetics as well as the absorption capacity of the material at much lower temperatures through the incorporation of germanium in lithium silicate.

From the highlighted dynamic thermogram (Fig. 9), it can be observed that the absorption is initiated from the lower temperature of 150 °C, and at temperatures above 250 °C, the absorption becomes significant. CO_2 absorption studies of the samples were also performed by heating the sample from ambient temperature to the respective absorption temperatures (300–680 °C) at a heating rate of 10 °C min^{-1} under 100% CO_2 flow. As expected, the absorption increased with the increase in temperature. The detailed absorption–desorption isotherms at various temperatures of the Ge-LS sample with the molar ratio of 1 : 0.183 are shown in Fig. 10.

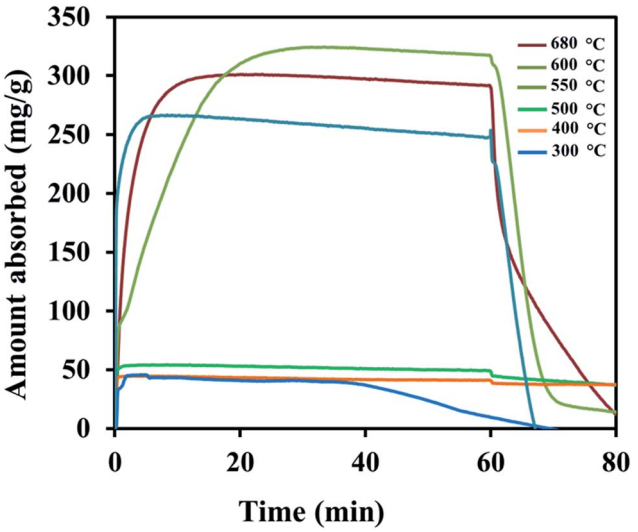

Fig. 10 A detailed comparison of the absorption performance of the synthesized Ge-LS sample in the molar ratio of 1 : 0.183, measured under isothermal conditions.

The sorption at higher temperatures was carried out by holding the sample at 550, 600 and 680 °C for one hour under 100% CO_2 gas flow, and complete desorption was obtained by switching the gas to N_2. At lower temperatures (300–500 °C), the sample was held for one hour under 100% CO_2 flow, and the desorption was attained by heating the sample to higher temperatures (700 °C), as switching the gas to N_2 alone at the absorption temperatures did not facilitate desorption of CO_2.

The absorption capacity of the 1 : 0.183 sample reached the maximum value of 320 mg g^{-1} at 600 °C within 25 min of CO_2 flow, and complete desorption was realized by switching the gas to N_2 at the same temperature. The absorption capacity was slightly lower (300 mg g^{-1}) at the measurement temperature of 680 °C, although the maximum capacity was attained much earlier with faster absorption kinetics. Complete desorption was also achieved at this temperature by switching the gas to N_2. The sample at 300 °C reached its maximum absorption capacity of 49 mg g^{-1} within 6 minutes of CO_2 exposure. This value increased only slightly even at the measurement temperature of 500 °C. However, desorption could not be achieved by switching the gas to N_2 at the measurement temperatures of 300 °C, 400 °C, or 500 °C. The desorption in such cases was realized by increasing the temperature to 700 °C. The full isotherm for a sample at 300 °C adsorption temperature and 700 °C desorption temperature is shown as a typical example in Fig. 10.

In order to elucidate the CO_2 sorption mechanism of the Ge-LS samples, the phase identification of the sorption products at 300 °C, 500 °C, 600 °C, and 680 °C was carried out using XRD analysis, as shown in Fig. 11. The characterization data show that the Ge-LS samples at T > 300 °C contained lithium carbonate and Li_2GeO_3 as sorption products, indicating the conversion of Ge-LS samples at temperatures as low as 300 °C. Upon increasing the temperature from 300 °C to 680 °C, the lithium orthosilicate phase diminishes, and an increase in the intensity of the lithium metasilicate phase was observed. The

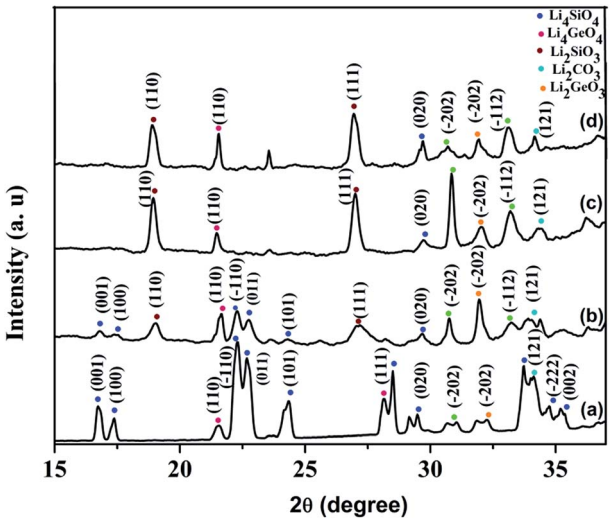

Fig. 11 X-ray diffraction patterns of germanium-incorporated lithium silicate after CO_2 sorption at (a) 300 °C, (b) 500 °C, (c) 600 °C, and (d) 680 °C.

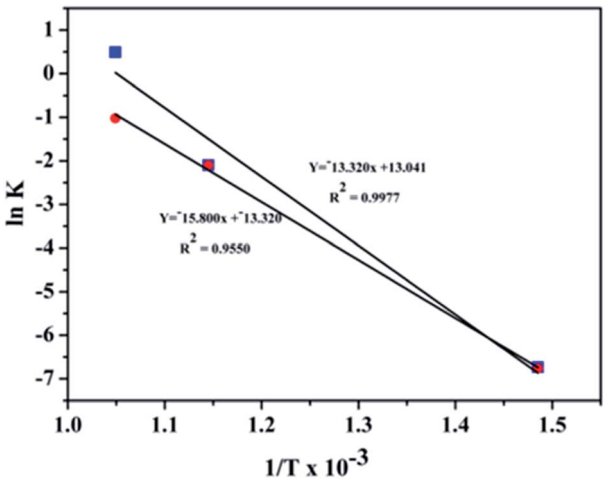

Fig. 13 The plot of ln K *versus* $1/T$ for the two different processes of chemisorption (K_1) and diffusion (K_2) observed on the germanium composite.

presence of the Li_2GeO_3 phase but not Li_2SiO_3 in the sorption products at 300 °C confirms the role of germanium in low-temperature CO_2 absorption.

The absorption rate at different temperatures was measured from the data in Fig. 12 and is shown in Fig. 13. Ge-LS samples showed absorption rate values of 36 mg g^{-1} min^{-1} and 44 mg g^{-1} min^{-1} at the low temperatures of 300 °C and 400 °C, respectively. At 500 °C, 600 °C, and 680 °C, the calculated absorption rates were 52, 91, and 118 mg g^{-1} min^{-1}, respectively, for this sample. The absorption rates were determined by calculating the absorption capacity within one minute in all cases. These observations clearly indicated that the Ge-LS samples exhibited enhanced kinetics similar to that of the pure LS sample but at low as well as elevated temperatures.

Different models have been proposed in the literature to understand the kinetic behaviour of the CO_2 chemisorption process. The kinetic calculations were performed on the absorption isotherms of the 1 : 0.183 (Si : Ge) sample at different temperatures and by fitting the curves with the well-accepted double exponential model.[22] The isotherms at various temperatures are fitted with the equation:

$$Y = A\exp^{-K_1 x} + B\exp^{-K_2 x} + C$$

where Y indicates the amount of CO_2 absorbed at time x and K_1, K_2 are exponential constants for the CO_2 chemisorption produced directly over the particles and the CO_2 chemisorption kinetically controlled by diffusion processes, respectively. We assume that chemisorption and diffusion occur during the sorption process. In the chemisorption process, the Li atoms on the surface of the sorbent react with CO_2 to form a Li_2CO_3 shell over the sorbent particle. In the diffusion process, the sorption completely relies on the diffusion of Li from the core of the material to the surface of the particle. The K_1, K_2 values calculated for the sample are listed in Table 2. The activation energy values for the measured samples were calculated as 131.36 kJ mol^{-1} for the chemisorption process and 110.57 kJ mol^{-1} for the diffusion process (Fig. 13). The higher activation energy value for the chemisorption process confirmed higher absorption of CO_2 by the surface reaction with lithium silicate particles.

One-cycle regenerability of the sample at 300 °C, 600 °C, and 680 °C is shown in Fig. 10. The cyclic absorption–desorption

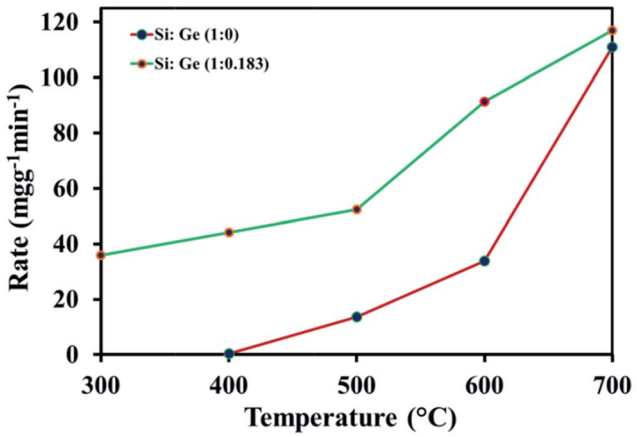

Fig. 12 Absorption rate of Si : Ge (1 : 0) and Si : Ge (1 : 0.183) samples at different temperatures.

Table 2 Kinetic parameters obtained from the isotherms of composites at different temperatures fitted to a double exponential model

Kinetic parameters of the Ge-LS sample (1 : 0.183)			
Temperature (K)	K_1 (s^{-1})	K_2 (s^{-1})	R^2
673	0.0011	0.0011	0.999
873	0.1227	0.1227	0.987
953	1.6368	0.3608	0.994

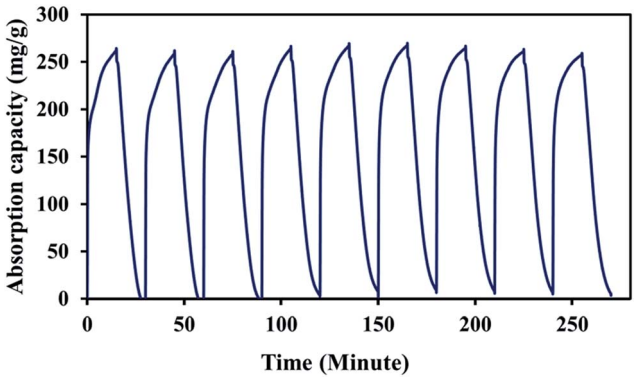

Fig. 14 Cyclic absorption–desorption results of the Ge-LS sample with the molar ratio of 1 : 0.183 at 550 °C. Desorption was carried out at the same temperature by changing 100% CO_2 to 100% N_2 gas.

data of the Ge-LS sample (of the molar ratio of 1 : 0.183) at 550 °C was also carried out and is shown in Fig. 14. The measurement was carried out at a static temperature of 550 °C by switching between 100% CO_2 and 100% N_2. From the cyclic measurement data, it can be observed that the sample shows no reduction in the original absorption capacity even after 9 cycles.

The current study thus indicates the possibility of employing germanium-incorporated lithium silicate for the low-temperature absorption of CO_2 at temperatures as low as 150 °C. Samples having a Si : Ge molar ratio of 1 : 0.183 exhibited an enhanced CO_2 absorption capacity as well as kinetics in the temperature range of 200–680 °C compared to pure Li_4SiO_4 absorbents. Due to their excellent performance in capacity and kinetics, the samples may find use in facilitating CO_2 sorption during the water–gas shift reaction as well as other petrochemical reactions in the temperature range of 300–400 °C. The current study thus provides a facile synthetic pathway to realize a ceramic sorbent that displays favourable kinetics at low and high-temperature ranges (150–680 °C) without the use of any eutectic additives.

4. Conclusions

In summary, germanium-incorporated lithium silicates synthesised *via* a microwave-assisted sol–gel process displayed enhanced CO_2 absorption capacity as well as kinetics in the temperature range of 150–680 °C compared to pure Li_4SiO_4 absorbents. The needle-shaped morphology of the synthesised particles coupled with the presence of germanium significantly altered the absorption kinetics of the material. An absorption capacity of 324 mg g^{-1} at a rate of 117 mg g^{-1} was attained at 680 °C for the samples with the Si : Ge molar ratio of 1 : 0.183. Moreover, an appreciable capacity of 49 mg g^{-1} at the rate of 36 mg g^{-1} min^{-1} was obtained at temperatures as low as 300 °C. This study thus indicates the possibility of employing germanium-incorporated lithium silicate for the *in situ* removal of CO_2 from reactive environments such as the water–gas shift reaction in the temperature range of 150–450 °C.

Conflicts of interest

There are no conflicts to declare.

Acknowledgements

We acknowledge the Council of Scientific and Industrial Research (CSIR), New Delhi, India, and Noritake Co. Limited, Aichi, Japan, for providing research facilities and financial support (CLP 218739). Dr Bhoje Gowd and Mr N. Prithviraj are acknowledged for the XRD measurements. Mr Kiran Mohan and Harish Raj V. are acknowledged for the TEM and SEM microscopy. Dr K. K. Maiti is gratefully acknowledged for the Raman spectral analysis.

Notes and references

1 D. M. D'Alessandro, B. Smit and J. R. Long, *Angew. Chem., Int. Ed.*, 2010, **49**, 6058–6082.
2 B. N. Nair, R. P. Burwood, V. J. Goh and K. Nakagawa, *Prog. Mater. Sci.*, 2009, **54**, 511–541.
3 K. Nakagawa and T. J. Ohashi, *J. Electrochem. Soc.*, 1998, **145**, 1344–1346.
4 J. Wang, L. Huang, R. Yang, Z. Zhang, J. Wu, Y. Gao, Q. Wang, D. O'Hare and Z. Zhong, *Energy Environ. Sci.*, 2014, **7**, 3478–3518.
5 X. W. Yang, W. Q. Liu, J. Sun, Y. C. Hu, W. Y. Wang, H. Q. Chen, Y. Zhang, X. Li and M. H. Xu, *Chemsuschem*, 2016, **9**, 2480–2487.
6 J. Ortiz-Landeros, I. C. Romero-Ibarra, C. Gomez-Yanez, E. Lima and H. Pfeiffer, *J. Phys. Chem. C*, 2013, **117**, 6303–6311.
7 Y. Duan, H. Pfeiffer, B. Li, I. C. Romero-Ibarra, D. C. Sorescu, D. R. Luebke and J. W. Halley, *Phys. Chem. Chem. Phys.*, 2013, **15**, 13538–13558.
8 S. Xiang, Y. He, Z. Zhang, H. Wu, W. Zhou, R. Krishna and B. Chen, *Nat. Commun.*, 2012, **3**, 954.
9 D. Y. C. Leung, G. Caramanna and M. M. Maroto-Valer, *Renewable Sustainable Energy Rev.*, 2014, **39**, 426–443.
10 S. Mane, Z. Gao, Y. Li, D. Xue, X. Liu and L. Sun, *J. Mater. Chem. A*, 2017, **5**, 23310–23318.
11 J. Geng, D. Xue, X. Liu, Y. Shi and L. Sun, *AIChE J.*, 2017, **63**, 1648–1658.
12 N. Minju, B. N. Nair, A. Peer Mohamed and S. Ananthakumar, *Sep. Purif. Technol.*, 2017, **181**, 192–200.
13 M. Thomas, B. N. Nair, G. M. Anilkumar, A. P. Mohamed, K. G. K. Warrier and U. S. Hareesh, *J. Environ. Chem. Eng.*, 2016, **4**, 1442–1450.
14 C. C. Wei, G. Puxty and P. Feron, *Chem. Eng. Sci.*, 2014, **107**, 218–226.
15 M. Midhun, T. Suzuki, K. N. Akhil, P. Saju, K. G. K. Warrier, U. S. Hareesh, B. N. Nair and J. D. Gale, *Phys. Chem. Chem. Phys.*, 2017, **19**, 25564–25573.
16 S. Jana, S. Das, C. Ghosh, A. Maity and M. Pradhan, *Sci. Rep.*, 2015, **5**, 1–9.
17 H. A. Mosqueda, C. Vazquez, P. Bosch and H. Pfeiffer, *Chem. Mater.*, 2006, **18**, 2307–2310.

18 K. Essaki, K. Nakagawa, M. Kato and H. J. Uemoto, *J. Chem. Eng. Jpn.*, 2004, **40**, 829–833.
19 Y. S. Shan, Q. M. Jia, L. H. Jiang, Q. C. Li and Y. M. Wang, *Chin. Sci. Bull.*, 2012, **57**, 2475–2479.
20 V. L. MejiÌa-Trejo and E. Fregoso-Israel, *Chem. Mater.*, 2008, **20**, 7171–7176.
21 R. RodrÃguez-Mosqueda and H. Pfeiffer, *J. Phys. Chem. A*, 2010, **114**, 4535–4541.
22 J. H. Lee, B. Moon, T. K. Kim, S. Jeoung and H. R. Moon, *Dalton Trans.*, 2015, **44**, 15130–15134.
23 Y. R. Pan, Y. Zhang, T. T. Zhou, B. Louis, D. O'Hare and Q. Wang, *Inorg. Chem.*, 2017, **56**, 7821–7834.
24 H. Pfeiffer, P. Bosch and S. Bulbulian, Synthesis of lithium silicates, *J. Nucl. Mater.*, 1998, **257**, 309–317.
25 M. J. Venegas, E. Fregoso-Israel, R. Escamilla and H. Pfeiffer, *Ind. Eng. Chem. Res.*, 2007, **46**, 2407–2412.
26 A. Nambo, J. He, T. Q. Nguyen, V. Atla, T. Druffel and M. Sunkara, *Nano Lett.*, 2017, **17**, 3327–3333.
27 T. Yamaguchi, T. Niitsuma, B. N. Nair and K. Nakagawa, *J. Membr. Sci.*, 2007, **294**, 16–21.
28 B. N Nair, K. Keizer, T. Okubo and S. I. Nakao, *Adv. Mater.*, 1998, **10**, 249–252.
29 V. Kumar, J. H. Kim, J. B. Jasinski, E. L. Clark and M. K. Sunkara, *Cryst. Growth Des.*, 2011, **11**, 2913–2919.
30 T. Q. Nguyen, V. Atla, V. K. Vendra, A. K. Thapa, J. B. Jasinski, T. L. Druffel and M. K. Sunkara, *Chem. Eng. Sci.*, 2016, **154**, 20–26.
31 P. V. Subha, B. N. Nair, P. Hareesh, A. P. Mohamed, T. Yamaguchi, K. G. K. Warrier and U. S. Hareesh, *J. Mater. Chem. A*, 2014, **2**, 12792–12798.
32 P. V. Subha, B. N. Nair, P. Hareesh, A. P. Mohamed, T. Yamaguchi, K. G. K. Warrier and U. S. Hareesh, *J. Phys. Chem. C*, 2015, **119**, 5319–5326.
33 J. C. Severiens and C. S. Fuller, *Phys. Rev.*, 1953, **92**, 1322–1323.
34 J. Graetz, C. C. Ahn, R. Yazami and B. Fultz, *J. Electrochem. Soc.*, 2004, **151**, A698–A702.
35 N. Togashi, T. Okumura and K. Ohnishi, Synthesis and CO_2 absorption property of Li_4TiO_4 as a novel CO_2 absorbent, *J. Ceram. Soc. Jpn.*, 2007, **115**, 324–328.
36 P. V. Subha, B. N. Nair, A. P. Mohamed, G. M. Anilkumar, K. G. K. Warrier, T. Yamaguchi and U. S. Hareesh, *J. Mater. Chem. A*, 2016, **4**, 16928–16935.
37 M. T. Izquierdoa, A. Turana, S. Garcíaa and M. M. Maroto-Valer, *J. Mater. Chem. A*, 2018, **6**, 3249–3257.
38 V. A. Efremov, V. N. Potolokov, S. V. Nikolashin and V. A. Fedorov, *Inorg. Mater.*, 2002, **38**, 847–853.
39 J. F. Watts, Analysis of ceramic materials by electron spectroscopy, *J. Microsc.*, 1985, **140**, 243–260.